Correlated defect creation and dose-dependent radiation sensitivity in amorphous SiO_2

R. A. B. Devine
Centre National d'Etudes des Télécommunications, Boîte Postale 98, 38243 Meylan CEDEX, France

J. Arndt
Mineralogisches Institut, Universität Tübingen, D-7400 Tübingen, Federal Republic of Germany
(Received 31 August 1988)

Electron-spin-resonance studies have been made of the kinetics of γ-ray-induced defect creation in samples of undensified, low-OH-concentration (<5 ppm) and high-OH-concentration (>1200 ppm) silica and in samples plastically densified by 12.3% (low OH) and 13.8% (high OH). For the oxygen-vacancy defect, E_1', creation is enhanced by a factor ~ 350 for high-OH-concentration samples and by ~ 200 for low-OH-concentration samples for a dose of 0.2 Mrad after densification. Nonbridging oxygen-hole center defect creation in high-OH-concentration silica is enhanced by ~ 50 times, essentially independent of γ-ray dose for the range studied (<8 Mrad). Arguments are advanced for a process of correlated defect creation via strained-bond cleavage in densified silica, while in undensified silica defects are created by radiolysis of OH bonds and oxygen displacement through ionizing-energy-related processes. It is concluded that the E_1' defects observed in densified silica are consequently only the paramagnetic part of the usual oxygen-vacancy defect.

INTRODUCTION

Although there are presently no experiments which permit one to study the short-range order in amorphous SiO_2 on a microscopic scale, it is generally accepted[1] that the material is composed of ring networks of SiO_2 tetrahedra which link in such a way as to produce[2,3] a distribution of intertetrahedral Si—O—Si bond angles whose mean is about 144°. This angle corresponds to that at which calculation[4] predicts the bond energy per SiO_2 molecule to be minimized. Regular ring structures are well known[5] in crystalline SiO_2 polymorphs and are thus expected to occur naturally in an extension to the amorphous phase. This extension is supported by an explanation of the origin of "defect lines" observed[6] in the Raman spectrum of amorphous SiO_2 which may be elegantly described[7] in terms of three- and four-membered rings in the network. Confirmation of the theoretical model for the Raman spectrum has been found recently from experiments[8] on sol-gel materials. These results suggest that low-order rings are present in bulk, amorphous SiO_2, but that their numbers are small, as one might expect on the basis of bond-angle and bond-energy arguments—thus adding weight to the hypothesis that the more energetically favorable, high-order rings are surely present and form the dominant constituent of the amorphous network.

One of the interesting physical properties of amorphous SiO_2 is the "plastic" densification produced by either large hydrostatic pressures[9] (>8 GPa at room temperature) or a combination of high pressure and temperature.[10] These densifications, which can easily attain 30% in volume, may be relaxed only by heating to high temperature ($>900\,^{\circ}C$). Densified, amorphous SiO_2 may also be grown[11] thermally on Si substrates by low-temperature processing ($T<800\,^{\circ}C$) or deposited by chemical-vapor deposition[12,13] from the decomposition of SiH_4 with N_2O. Although the detailed mechanism of densification remains unexplained, comparison of the mean Si—O—Si bond-angle variation with densification[14] deduced for elastically densified single-crystal quartz and bulk, amorphous SiO_2 and plastically densified amorphous SiO_2 indicates that the variation is approximately 2.5 times larger in the elastic case. This strongly suggests that the amorphous phase accommodates a significant volume decrease by modifying its internal structure while maintaining the mean Si—O—Si bond angle as least shifted as possible from the value at which the bond energy per molecule is minimized. The simplest interpretation of these results is to assume that the large rings in the network "cleave" to produce smaller rings (hence smaller volume occupied) while maintaining the Si—O—Si bond angle close to 144°. The mechanism of ring cleavage remains open since, although the energy per SiO_2 molecule varies little from low-order rings to high-order rings[15] (the rings can always pucker or planarize to reduce their energy), the energy barrier to ring division and rebonding is unknown, although it may be considerably less than the energy for Si—O bond breaking.[16]

With the objective of obtaining some information on the internal structure of amorphous SiO_2, we have carried out[17,18] electron-spin-resonance (ESR) studies on paramagnetic defects created in densified, amorphous SiO_2 by ^{60}Co γ radiation. It appears that the defects studied, the oxygen-vacancy (E_1') center, nonbridging oxygen-hole center (NBOHC), and peroxy radical, all have electron spins which are too localized spatially to be useful "monitors" of the structure of their amorphous environment.[19] However, some information can be retrieved from studies of the defect growth and/or annihi-

 ©1989 The American Physical Society

lation kinetics. In particular, the E'_1 center can anneal by trapping a diffusing O_2 molecule to produce a peroxy radical:[20]

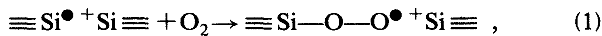

$$\equiv Si^{\bullet}\ {}^{+}Si\equiv + O_2 \rightarrow \equiv Si—O—O^{\bullet}\ {}^{+}Si\equiv \ , \qquad (1)$$

where $\equiv Si^{\bullet}\ {}^{+}Si\equiv$ is the E'_1 center and $\equiv Si—O—O^{\bullet}$ the peroxy radical. (The charge balance is assumed; to our knowledge no experimental evidence exists to prove or disprove the equality when peroxy radicals are formed.) In consequence, a study of E'_1 annealing via peroxy-radical formation can be used as a potential monitor of O_2 diffusion. In undensified silica, despite uncertainties in the appropriate choice of annealing model, values[21] for the diffusion coefficient of O_2 in reasonable agreement with known values have been extracted.[22] Similar measurements[17] on densified, amorphous SiO_2 have enabled us for the first time to obtain clear evidence for a significant reduction in the O_2 diffusion coefficient due to densification. This phenomenon has been frequently cited[23] in models for the diffusion-limited oxidation of Si where interfacial stress is suggested to limit O_2 diffusion and hence the oxidation rate at the Si surface.

In previous studies on densified, amorphous SiO_2, we concentrated[17,18] on defects created by a fixed dose of ^{60}Co γ rays and examined the defect creation and annihilation as a function of densification. We have extended this work and studied defect creation in samples of fixed densification ($\sim 10\%$) as a function of γ dose. We have also studied the dose-dependent defect creation in undensified samples of SiO_2 (both low and high OH concentration) for comparative purposes. The results of these studies are reported in the following.

EXPERIMENTAL METHODS AND RESULTS

Experiments were carried out on bulk samples of Suprasil I (> 1200 ppm OH) and Suprasil W1 (< 5 ppm OH), both obtained from the Hereaus company. Densified samples were made using a belt apparatus (described previously[10]) by subjecting a sample of Suprasil I to a pressure of 5 GPa at 600 °C for 3 min and a Suprasil W1 sample to 5 GPa at 500 °C for 10 min. AgCl was used as the pressure-transmitting medium. Density increases, as ascertained by the flotation method and verified by refractive-index measurements,[10] were 13.8% for the Suprasil I and 12.3% for the Suprasil W1. Samples were subsequently broken into small pieces and irradiated simultaneously with undensified, bulk samples in a ^{60}Co γ source at a rate of 0.33 Mrad/h. Accumulated doses up to a maximum ~ 7.7 Mrad were used. Immediately subsequent to irradiation, samples were stored in a liquid-nitrogen storage vessel where they remained until a few minutes prior to measurement. ESR measurements were carried out using a Bruker ER 200 D X-band spectrometer using a magnetic-field-modulation frequency of 100 kHz. In common with previous experiments, a Cr in the MgO reference sample was installed permanently in the microwave cavity to monitor possible fluctuations in spectrometer performance occurring during the experiments. Oxygen-vacancy (E'_1) spectra were measured at

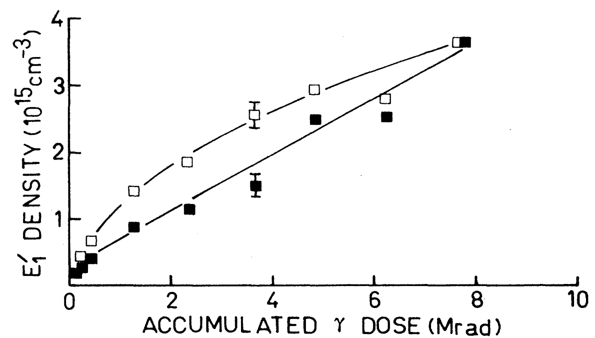

FIG. 1. Variation of the E'_1 density with accumulated γ dose in undensified Suprasil I (■) and undensified Suprasil W1 (□).

room temperature using nonsaturating microwave-power levels (< 0.2 μW) and magnetic-field-modulation amplitudes ~ 0.125 G. Nonbridging oxygen-hole-center spectra were obtained at a sample temperature of 120 K using microwave-power levels 2 mW and field-modulation amplitudes of 1.25 G. We confirmed that under these conditions the NBOHC spectrum showed no signs of saturation. Determination of the absolute density of defects was carried out by comparison of the resonance spectrum with that of a standard strong-pitch sample using a double-integration method to obtain the area under the resonant-absorption curve.[24]

In Fig. 1 we show the results obtained for the growth of the E'_1 defect density in undensified Suprasil W1 and Suprasil I as a function of accumulated γ dose. The y scale indicates the spin density determined by double integration and comparison with the pitch standard. We observe that the defect densities created in Suprasil I and Suprasil W1 are approximately equal for a γ dose of 7 Mrad, which is consistent with higher-dose data obtained previously.[25] At low doses, E'_1 defects are created less efficiently in high-OH-concentration silica than in the case of low concentration. In Fig. 2 we show the results obtained for E'_1 creation in the densified samples. Over

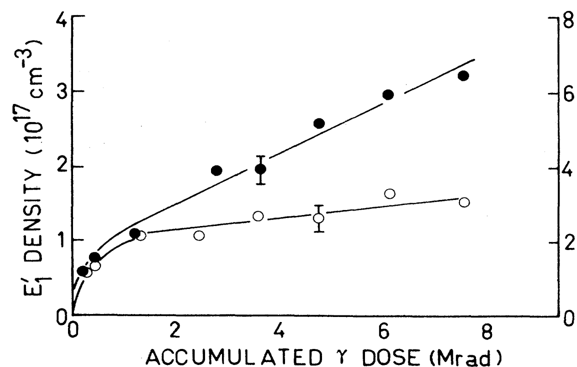

FIG. 2. Variation of the E'_1 density with accumulated γ dose in a sample of Suprasil I densified by 13.8% (●) and a sample of Suprasil W1 densified by 12.3% (○).

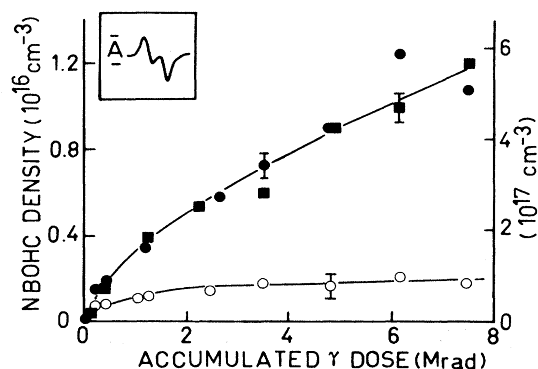

FIG. 3. Variation of the NBOH-center density with accumulated γ dose in a sample of Suprasil W1 densified by 12.3% (○), a sample of Suprasil I densified by 13.8% (●), and an undensified Suprasil I sample (■). Note that the right-hand scale applies to the densified samples, while the left-hand scale is for the undensified sample. The measured parameter, A, shown in the inset, is that used to characterize the NBOHC-defect density.

the entire dose range measured, E_1' defects are created more efficiently in high-OH-concentration silica than in low-OH-concentration silica—note that the vertical scale is increased $\sim$200 times with respect to that of Fig. 1.

The results obtained for the NBOHC are shown in Fig. 3. Because of the interference of the E_1' spectrum with that of the NBOHC, it was not, in general, possible to ascertain the NBOHC defect density by the double-integration–pitch comparison method. For this reason it was decided to use the amplitude A (see inset, Fig. 3) of the positive maximum–negative minimum excursion of the NBOHC signal as an indication of the relative behavior of the defect density. Caution must be exercised in interpreting Fig. 3 since full account was not taken of possible (undetectable) variations in the resonance line shape masked by the E_1' signal. However, measurements of the peak width at half-positive peak height indicated no detectable variation either as a function of γ dose or as a function of densification. The results presented in Fig. 3 should, with this reserve, be a reasonable approximation to the actual defect densities. Note that in undensified Suprasil W1 the presence of the large peroxy-radical resonance signal prohibits any estimation of the NBOHC density. This signal is, fortunately, absent in densified[17] Suprasil W1.

DISCUSSION

E_1' and NBOH centers

The results presented in Figs. 1 and 2 are plotted together with other available data in Fig. 4 on a log-log scale. For the case of γ doses < 1000 Mrad the low-OH-concentration data can be fitted by power laws of the form

$$n_{E'}=(1.3\times10^{15})D^{0.30} \quad (12.3\%\ \text{densified W1}) , \tag{2}$$

$$n_{E'}=(3.2\times10^{11})D^{0.58} \quad (\text{undensified W1}) , \tag{3}$$

where D is the γ dose in rad. For high-OH-concentration Suprasil I in the same dose range, we obtain

$$n_{E'}=(2.6\times10^{14})D^{0.49} \quad (13.8\%\ \text{densified I}) , \tag{4}$$

$$n_{E'}=(2.9\times10^{10})D^{0.77} \quad (\text{undensified W1}) . \tag{5}$$

We recall that the densified data are over a much more restricted dose range (<2 decades), whereas the undensified data are over $\sim$4 decades of dose. At high dose in thermally grown low-OH-concentration oxide, data obtained by low-energy electron irradiation[26] indicate that the E_1' defect density grows linearily with dose, while in the high-OH-concentration thermal oxide the same radiation produces defects with a power law of the form $D^{0.36}$. The reduction in exponent from the low-dose value may be indicative of the onset of a saturation in the defect density. Indeed, E_1' densities in this regime are

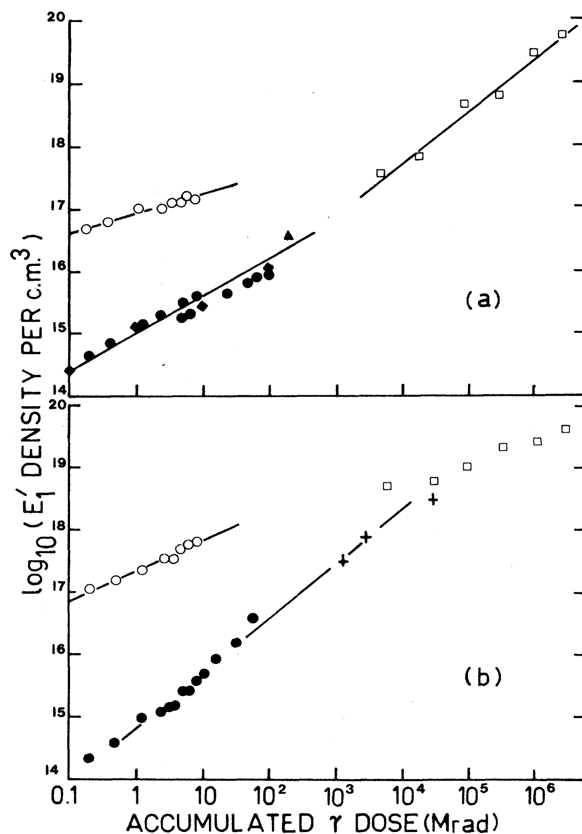

FIG. 4. Compilation of data on E_1'-defect creation as a function of accumulated γ dose in Suprasil W1 and low-OH-concentration silica samples [panel (a)] and Suprasil I and high-OH-concentration silica samples [panel (b)]. The open circles apply to the densified data shown in Fig. 2, while the solid circles are taken from Fig. 1 and Ref. 25. Other data points are as follows: □, Ref. 26; ♦, Ref. 27; ▲, Ref. 28; and +, Ref. 29.

$\sim 10^{20}$ cm^{-3}, which is of the same order as that found for the saturation value of defect creation when particle radiation is used,[30] and where the prime mechanism of energy loss is via atomic collisions and displacements rather than ionizing energy loss, as in the case of electron, γ, or proton radiation. The smaller exponents observed in *densified* Suprasil I and W1 [Eqs. (2) and (4)] as compared to undensified values cannot be indicative of saturation in the same sense since the changes are observed for defect densities which are nearly 2 orders of magnitude smaller than those where saturation is suggested in the undensified case.

^{60}Co γ rays are of sufficient energy to produce Compton electrons having an energy ~ 1 MeV. Since the threshold for displacement of an oxygen atom in SiO_2 by an energetic electron is 150 keV, 1-MeV electrons are clearly capable of creating oxygen vacancies by direct displacement. Assuming a typical dose of 10 Mrad and that all the γ rays create Compton electrons, one can demonstrate[31] that the maximum number of displaced oxygens, n_O, in SiO_2, per cm^3, is $3\times 10^{15} < n_O < 6\times 10^{15}$. If in displacement collisions only $\frac{1}{37}$ of displaced oxygens result in a permanent oxygen vacancy,[32] then 10 Mrad of ^{60}Co γ rays will produce a maximum number of E_1' defects, $n_{E'}$, per cm^3, of $8\times 10^{13} < n_{E'} < 1.6\times 10^{14}$. Comparison of these figures with the results shown in Fig. 4 show that even for undensified samples a dose of 10 Mrad produces $(4\times 10^{15})E_1'$ in undensified Suprasil W1 and 6×10^{15} in Suprasil I. These densities are significantly larger than those expected if displacement collisions due to Compton electrons were the dominant mechanism of defect creation. One can then reasonably assume that it is the energy loss by the γ ray in processes such as electron-hole–pair creation that subsequently results in defect creation. At the present time we have no indication of the density of E_1' precursors (for example, B_2 centers) which might also be transformed by ionizing radiation. Given the apparent validity of the power law in γ dose demonstrated in Fig. 4 down to defect densities of $\sim 2\times 10^{14}$ cm^{-3}, this might suggest that the density of defects produced by precursor transformation is probably $< 10^{14}$ cm^{-3}.

In undensified Suprasil I we observe that E_1' centers are centered with a dose dependence $D^{0.77}$, while in Suprasil W1 the law is $D^{0.58}$. Characteristically, we observe that in Suprasil W1 γ radiation at room temperature produces both E_1' and peroxy-radical defects, while there is almost no peroxy creation in Suprasil I. From Eq. (1) this suggests that in Suprasil W1 there is some form of E_1' "self-annealing" occurring during the irradiation process. One can naively model the E_1' defect-creation and -annihilation process using a simple approach to the rates of creation and annihilation with γ dose:

$$dN_c/dD = \sigma_c(N_0 - N) \ , \tag{6}$$

$$dN_a/dD = \sigma_a N + \sigma_{E\text{-}p} N \ , \tag{7}$$

where N_0 is the maximum available number of E_1' sites, σ_c and σ_a are cross sections for E_1' creation and annihilation, and $\sigma_{E\text{-}p}$ is a cross section for transformation of E_1' defects into peroxy radicals. Solution of Eqs. (6) and (7) leads to a dose-dependent E_1' density growth of the form

$$N = \frac{\sigma_c N_0}{\sigma_c + \sigma_a + \sigma_{E\text{-}p}} \{1 - \exp[-(\sigma_c + \sigma_a + \sigma_{E\text{-}p})D]\} \ . \tag{8}$$

Since the $\sigma_{E\text{-}p}$ term is absent for the case of Suprasil I, one can expect the E_1' density to rise more rapidly with γ dose for this case than for Suprasil W1 as is observed for undensified silica. However, a reduced rate of growth is also observed for the case of densified Suprasil W1, where it is known that room-temperature irradiation does not give rise to peroxy-radical generation. Furthermore, comparison of the exponents of the power-law equations (2)–(5) yields

$$n_{E'}(\text{Suprasil I})/n_{E'}(\text{Suprasil W1}) \sim D^{0.19}$$

for both the undensified and densified cases. Given the experimental accuracy and limited range of data for the densified material, the equality of the exponents for the two cases points to the fact that the origin of the difference in the original exponents may not be the role of peroxy generation, but rather a difference in the efficiency of the defect-creation process between the low- and high-OH-concentration silica. Since defect generation is assumed to be initially related to the creation of electron-hole pairs, which subsequently cause oxygen-vacancy creation via, perhaps, an excitonic mediary, we must assume that there are subtle differences either in the electron-hole–creation efficiency or in the excitonic lifetime[33] in the two types of silica.

In Fig. 5 we plot the NBOHC data of Fig. 3 on a logarithmic scale. The data, although over a limited γ-dose range, may be fitted by the equations

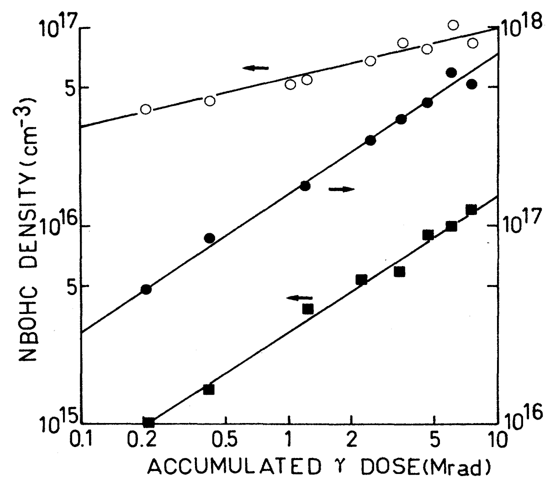

FIG. 5. Data for the NBOH-center creation as a function of γ dose taken from Fig. 3 and plotted on a logarithmic scale. ●, densified Suprasil I; ○, densified Suprasil W1; ■, undensified Suprasil I. Note that the right-hand scale applies to the densified Suprasil I sample.

$$n_{\mathrm{OHC}}=(9.11\times10^{12})D^{0.70} \quad (\text{densified I}) , \tag{9}$$

$$n_{\mathrm{OHC}}=(2.24\times10^{11})D^{0.69} \quad (\text{undensified I}) , \tag{10}$$

$$n_{\mathrm{OHC}}=(1.70\times10^{15})D^{0.25} \quad (\text{densified W1}) . \tag{11}$$

Given the experimental accuracy, it would appear that the same dose dependence is found for both densified and undensified Suprasil I.

It is generally assumed[34] that in high-OH-concentration silica, NBOH centers are created by the radiolysis of network OH linkages:

$$\equiv\mathrm{Si}\text{—}\mathrm{OH}+h\nu\rightarrow\equiv\mathrm{Si}\text{—}\mathrm{O}^{\bullet}+H^{0} . \tag{12}$$

It is then surprising at first sight that the defect-creation efficiency in densified Suprasil I is only ~6 times that observed in densified Suprasil W1, even though the OH content is >200 times larger. In Suprasil I the volume density of OH groups is of the order of 9×10^{19} cm^{-3}. From Fig. 5 we see that, for a γ dose of 1 Mrad, approximately 3×10^{15} NBOHC/cm^3 result in undensified Suprasil I, so that from Eq. (12) only $\sim3\times10^{-5}$ of the available OH groups are "permanently" transformed into defects. Again, from Fig. 5 this number apparently increases by 50 times in densified Suprasil I to 1.5×10^{-3}. One must comment that since the OH groups are terminations on SiO_4 tetrahedra backbonded by three Si—O—Si linkages into the network, it is not at all clear why densification should enhance the radiolysis of the OH bond, even though the experimental results appear to suggest this. Suprasil W1 contains $<4\times10^{17}$ OH/cm^3, so that if we assume that in the densified material 1.5×10^{-3} are transformed as in Suprasil I for a γ dose of 1 Mrad, then we conclude that we should observe $\sim6\times10^{14}$ NBOHC/cm^3. The results in Fig. 5 show that we, in fact, observe $\sim5\times10^{16}$ cm^{-3}, so that either the process of creation in significantly enhanced or NBOHC's are created via a different mechanism than radiolysis of Si—OH bonds. The results presented in Fig. 3 for E_1' creation in densified Suprasil W1 indicate that $n_{E'}=(1.3\times10^{15})D^{0.30}$. This equation is far too close to the NBOH-center form, $n_{\mathrm{OHC}}=(1.7\times10^{15})D^{0.25}$, to be coincidence. Such a correlation strongly suggests that E_1' and NBOHC defects are created simultaneously, and we believe that this result is consistent with a mechanism of creation involving strained bond cleavage. In undensified silica, the cleaving of one Si—O bond in a Si—O—Si link is likely to be followed by recombination since the Si—O—Si bond angle prior to cleavage was optimized to minimize the bond energy. In the densified form, severely strained bonds will exist since the whole network is in a state of metastable equilibrium brought about, we assume, by changes in the distribution in ring statistics. Once the strained bond is cleaved, the network may relax to a new equilibrium which does not necessarily involve recombination of the Si—O—Si linkage that has been opened:

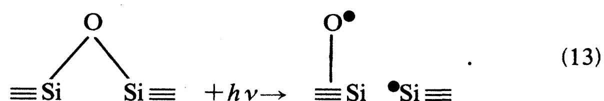

(13)

For the case of Suprasil I, for the dose range covered, we observe, in general, greater E_1'-defect–creation efficiency than NBOHC. This result may be consistent with the loss of a finite number of $\equiv$Si—O$^\bullet$ linkages, generated as in Eq. (13), by the subsequent trapping of radiolyzed hydrogen, i.e., the reverse reaction of Eq. (1), bearing in mind the very large OH content of Suprasil I.

Enhancement of defect creation

We compare the defect-creation efficiency in densified and undensified silica by defining two parameters, η and δ, such that

$$\eta=\left.\frac{E_1' \text{ density in densified silica}}{E_1' \text{ density in undensified silica}}\right|_{\text{same dose}} ,$$

and a similar form for δ, but for the NBOHC's. We plot in Fig. 6 these parameters as deduced from Figs. 1–3. In both high- and low-OH-concentration silica there is a rapid rise in η with decreasing dose for $D<0.8$ Mrad. For the lowest dose measured, 0.2 Mrad, η exceeds 350 for Suprasil I and 200 for Suprasil W1. Results for δ suggest that it is only slightly sensitive to γ dose and remains constant at ~50 for the dose range studied. From Eqs. (2)–(5) we obtain the approximate dose-dependent growth law for

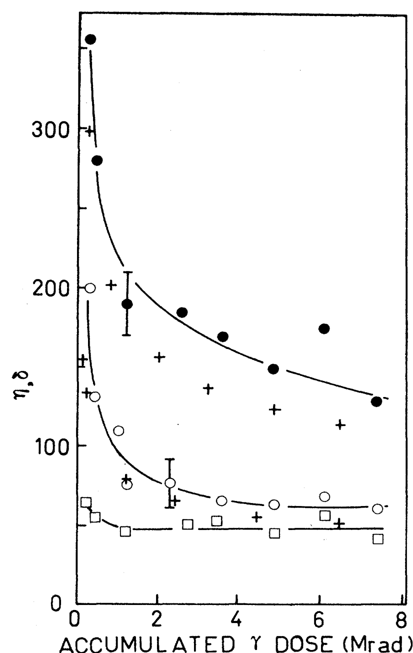

FIG. 6. Ratio of creation efficiencies, η, for E_1' defects and δ for NBOH centers in densified and undensified samples as a function of γ dose. ●, E_1' center, Suprasil I; ○, E_1' center, Suprasil W1; □, NBOH centers in Suprasil I. The plus symbols are the predictions based on the ratios of the power laws found for the growth of the defect densities in the different samples (see text).

$$\eta(\mathrm{I})=(8.9\times10^{3})D^{-0.28}\ , \quad (14)$$

$$\eta(\mathrm{W1})=(4.1\times10^{3})D^{-0.28}\ . \quad (15)$$

The predictions of these laws are shown by the plus symbols in Fig. 6. Deviations from the experimental curves reflect the errors in the initial power laws [Eqs. (2)–(5)] due to accuracy of the experimental points. It is intriguing that both types of silica have the same power law even though the four types of silica involved (undensified and densified) all had different individual power-law exponents. Such a result may be anticipated if, as suggested previously, the different dose dependence of E_1' creation simply represents a different efficiency for the γ ray in breaking Si—O bonds through electronic processes (direct excitation, electron-hole–pair relaxation, exciton relaxation, etc.) in the two types of silica. In undensified silica, two Si—O bonds must be broken to release an oxygen and create a vacancy, while in densified silica only one (strained) bond need be broken [Eq. (13)]. It is not, then, inconceivable that the appropriate ratios for these processes, taken for low- and high-OH-concentration silica, produce the same γ-dose power law.

CONCLUSIONS

The original objective of this work was to obtain information on the physical properties of plastically densified amorphous SiO_2. Neither of the defects we studied (E_1' or NBOHC) were observable in the densified or undensified silica prior to irradiation. We have argued that, for the doses we used (< 10 Mrad), the defect densities observed cannot be due to precursor transformation and consequently, we, deduce an upper limit of the number of precursors to be 10^{14} cm^{-3}.

The closely correlated growth of E_1' defects and NBOH centers in densified low-OH-concentration (Suprasil W1) silica strongly suggests that the defect densities we have observed, $\sim10^{17}$ cm^{-3}, are produced by the cleavage of strained Si—O—Si bonds which subsequently relax the network locally rather than the creation of oxygen vacancies by oxygen displacement or Si—O dangling bonds by the radiolysis of Si—OH groups. Similar arguments apply to high-OH-concentration silica, although there would appear to be some evidence that radiolyzed hydrogen does suppress some NBOH centers by forming OH bonds.

We have observed very large enhancements of the E_1'- and NBOHC-creation efficiency in densified material as compared to undensified silica, in qualitative agreement with the strained-bond-cleavage hypothesis. Such correlated creation should not result in the production of any form of charge, contrary to the usual situation for E_1' defects, which are positively charged. The E_1' centers we observed are thus assumed to be only the magnetic part of the usual E_1' defect. Support for these assumptions may come from recent magnetic and electrical measurements[35] on thin SiO_2 films deposited by plasma-enhanced chemical-vapor deposition that show anomalously large photoinduced E_1' defect creation without associated charge creation. Since as-deposited films such as these are typically in a state of $\sim5\%$ densification,[13] it would appear that the photoinduced E_1' defects may result from strained-bond cleavage.

Note added. Dr. Akos Revesz has reminded us that even in undensified silica, naturally occurring strained bonds are present which could produce E_1' and NBOH defects by the strained-bond-cleavage approach we have hypothesized. Such bonds could be construed to be "precursors" of the defects in the same way as the doubly occupied oxygen vacancies (B_2 centers) and OH terminations ($\equiv$Si—OH). In any event, the permanent E_1'-defect concentration in undensified silica resulting from all precursor transformation by γ radiation appears to be less than 2×10^{14} cm^{-3}.

ACKNOWLEDGMENTS

This work was supported in part by North Atlantic Treaty Organization International Collaboration Grant No. 87/18. We gratefully acknowledge constructive comments made by Dr. A. G. Revesz.

[1]See, for example, F. L. Galeener, in *The Physics and Technology of Amorphous SiO₂*, edited by R. A. B. Devine (Plenum, New York, 1988), p. 1 and references therein.
[2]R. Dupree and R. F. Pettifer, Nature (London) **308**, 523 (1984).
[3]Y. T. Thathachari and W. A. Tiller, J. Appl. Phys. **53**, 8615 (1982).
[4]M. D. Newton and G. V. Gibbs, Phys. Chem. Mineral. **6**, 221 (1980).
[5]F. Liebau, in *The Physics and Technology and Amorphous SiO₂*, edited by R. A. B. Devine (Plenum, New York, 1988), p. 15.
[6]F. L. Galeener, J. Non-Cryst. Solids **49**, 53 (1982).
[7]F. L. Galeener, A. R. Barrio, E. Martinez, and R. J. Elliott, Phys. Rev. Lett. **53**, 2429 (1984).
[8]C. A. M. Mulder and A. A. J. M. Damen, J. Non-Cryst. Solids **93**, 387 (1987).
[9]R. J. Hemley, K. H. Mao, P. M. Bell, and B. O. Mysen, Phys. Rev. Lett. **57**, 747 (1986).
[10]J. Arndt and D. Stoffler, Phys. Chem. Glasses **10**, 117 (1969).
[11]E. A. Taft, J. Electrochem. Soc. **125**, 968 (1978).
[12]M. Huffman and P. McMillan, J. Non-Cryst. Solids. **76**, 369 (1985).
[13]M. D. Bruni, A. Tissier, F. Ferrieu, and R. A. B. Devine (unpublished).
[14]R. A. B. Devine, J. Vac. Technol. A **6**, 3154 (1988).
[15]F. L. Galeener, Solid State Commun. **44**, 1037 (1982).
[16]R. Jeanloz, Nature (London) **332**, 207 (1988).
[17]R. A. B. Devine, Phys. Rev. B **35**, 9783 (1987).
[18]R. A. B. Devine and J. Arndt, Phys. Rev. B **35**, 9376 (1987).
[19]D. L. Griscom and E. J. Friebele, Radiat. Effects **65**, 303 (1982).
[20]A. H, Edwards and W. B. Fowler, Phys. Rev. B **26**, 6649 (1982).
[21]R. Bruckner, J. Non-Cryst. Solids **5**, 123 (1970).
[22]R. A. B. Devine, Nucl. Instrum. Methods B **1**, 378 (1984).

[23]E. Kobeda and E. A. Irene, J. Vac. Sci. Technol. B **5**, 15 (1987).
[24]C. P. Poole, Jr., *Electron Spin Resonance* (Wiley, New York, 1983).
[25]R. A. B. Devine, J. Non-Cryst. Solids **107**, 41 (1988).
[26]R. L. Pfeffer, J. Appl. Phys. **57**, 5176 (1985).
[27]E. Dooryhee, Ph.D. thesis, University of Paris–Sud, 1987.
[28]C. L. Marquardt and G. H. Sigel, Jr., IEEE Trans. Nucl. Sci. **NS-22**, 2234 (1975).
[29]R. A. B. Devine, Appl. Phys. Lett. **43**, 1058 (1983).
[30]R. A. B. Devine and A. Golanski, J. Appl. Phys. **55**, 2738 (1984).
[31]O. S. Oen and D. K. Holmes, J. Appl. Phys. **30**, 1289 (1959).
[32]R. A. B. Devine (unpublished).
[33]K. Tanimura, T. Tanaka, and N. Itoh, Phys. Rev. Lett. **51**, 423 (1983).
[34]D. L. Griscom, in *Structure and Bonding in Non-Crystalline Solids,* edited by G. E. Walrafen and A. G. Revesz (Plenum, New York, 1986), p. 369.
[35]W. L. Warren, P. M. Lenahan, B. Robinson, and J. H. Stathis, Appl. Phys. Lett. **53**, 482 (1988).